

Confronting Grand Unification with Lepton Flavour Violation, Dark Matter and LHC Data

J. Ellis¹, M.E. Gómez², S. Lola³, R. Ruiz de Austri⁴, Q. Shafi⁵

¹ Theoretical Particle Physics and Cosmology Group, Department of Physics,
King's College London, Strand, London WC2R 2LS, UK;
National Institute of Chemical Physics & Biophysics, R vala 10, 10143 Tallinn, Estonia;
Theoretical Physics Department, CERN, CH-1211 Geneva 23, Switzerland

² Departamento de Ciencias Integradas y Centro de Estudios Avanzados en F sica Matem ticas y
Computaci n, Campus El Carmen, Universidad de Huelva, 21071 Huelva, Spain

³ Department of Physics, University of Patras, 26500 Patras, Greece

⁴ Instituto de F sica Corpuscular, IFIC-UV/CSIC, Valencia, Spain

⁵ Bartol Research Institute, Department of Physics and Astronomy, University of Delaware,
Newark, DE 19716, USA

ABSTRACT

We explore possible signatures for charged lepton flavour violation (LFV), sparticle discovery at the LHC and dark matter (DM) searches in grand unified theories (GUTs) based on SU(5), flipped SU(5) (FSU(5)) and SU(4)_c × SU(2)_L × SU(2)_R (4-2-2). We assume that soft supersymmetry-breaking terms preserve the group symmetry at some high input scale, and focus on the non-universal effects on different matter representations generated by gauge interactions at lower scales, as well as the charged LFV induced in Type-1 see-saw models of neutrino masses. We identify the different mechanisms that control the relic DM density in the various GUT models, and contrast their LFV and LHC signatures. The SU(5) and 4-2-2 models offer good detection prospects both at the LHC and in LFV searches, though with different LSP compositions, and the SU(5) and FSU(5) models offer LFV within the current reach. The 4-2-2 model allows chargino and gluino coannihilations with neutralinos, and the former offer good detection prospects for both the LHC and LFV, while gluino coannihilations lead to lower LFV rates. Our results indicate that LFV is a powerful tool that complements LHC and DM searches, providing significant insights into the sparticle spectra and neutrino mass parameters in different models.

1 Introduction

Experimental and theoretical considerations both require extending the Standard Model (SM) of particle physics, which can neither accommodate massive neutrinos, nor explain the observed baryon asymmetry of the universe, nor provide dark matter [1, 2, 3, 4]. Nevertheless, the data from the LHC [5, 6, 7, 8] and dark matter searches [9, 10, 11, 12, 13] have not yet yielded any positive signature of physics beyond the SM. On the contrary, severe constraints have been derived for the simplest extensions of the SM that address these issues, including the most simplified versions of supersymmetric unified theories. However, supersymmetry (SUSY) continues to have strong theoretical attraction and, among other features, provides a natural candidate for dark matter (DM) [14] and facilitates the construction of grand unified theories (GUTs) [15]. It is therefore premature to exclude SUSY before studying in more detail non-simplified models that have not yet been explored.

In doing so, flavour physics inevitably plays a crucial role, since it also provides severe bounds on extensions of the SM that would have resulted in exotic manifestations of flavour violation that have not yet been observed. In particular, supersymmetric theories have several possible sources of lepton flavour violation (LFV), which would yield unacceptably large effects unless off-diagonal entries in the sfermion mass matrices were small at some high scale. Even in this case, however, quantum corrections during the running from high scales to low energies would modify this simple structure. This effect is particularly significant in see-saw models for neutrino masses, where the Dirac neutrino Yukawa couplings cannot be diagonalised simultaneously with the charged (s)lepton Yukawa couplings [16]. In this case, the large mixing of neutrino families required by the data also implies that charged LFV may occur at enhanced rates for sufficiently small soft supersymmetry-breaking masses. This can occur in rare decays and conversions (e.g., $\mu \rightarrow e\gamma$ and $\tau \rightarrow \mu\gamma$, $\mu \rightarrow 3e$, $\tau \rightarrow e\gamma$ and $\mu - e$ conversion [17, 18]),¹ but also in other processes such as sparticle production at the LHC [20, 21, 22, 23, 24, 25, 26, 27] and slepton pair production at a Linear Collider (LC) [28, 29, 30, 31, 32, 33, 34, 35], particularly in the decays of the second-lightest neutralino.

In this paper we study the possibilities for LFV, LHC and dark matter searches in models with various grand unification groups. We pay particular attention to comparisons between their respective signatures, and to ways to differentiate between the various schemes in present and future searches. Since the SO(10) GUT model is now severely constrained by the data, we focus on GUTs based on SU(5), flipped SU(5) (FSU(5)) and SU(4)_c × SU(2)_L × SU(2)_R (4-2-2) [36, 37, 38]. Similarly to previous works within various GUT models [39, 40, 41, 42, 43, 44, 45], we assume that at the unification scale the soft SUSY-breaking terms preserve the group symmetry, and focus on the non-universal effects on different matter representations due to the gauge structures of the groups. We also include the charged LFV induced in these models via Type-1 see-saw models of neutrino masses with right-handed neutrinos at some high intermediate mass scale.

Different mechanisms that control the relic DM density in the various GUT models, lead to contrasting LFV and LHC signatures. Although the results are sensitive to the scale of the right-handed

¹For pioneering studies of $\mu \rightarrow e\gamma$ in supersymmetric models, see [19].

neutrinos (with larger scales being linked to larger couplings and thus larger flavour violation due to quantum corrections), for similar see-saw parameters, detailed comparisons between different unification schemes can be made. In all cases, coannihilations result to higher LFV rates. We find that the SU(5) and 4-2-2 models have different LSP compositions, but both offer good prospects for detection at both the LHC and in LFV searches. The FSU(5) model also offers LFV within the current reach, for instance in stop and stau coannihilation scenarios. The 4-2-2 model admits novel DM mechanisms such as chargino and gluino coannihilations with neutralinos. The former offers good detection prospects for both the LHC and LFV, whereas gluino coannihilations lead to lower LFV rates, and Higgsino DM models do not predict detectable LFV. In addition, we derive specific correlations between the respective sparticle spectra, providing further input on the experimental signatures that can be expected in each scheme, commenting on the prospects for direct detection of DM as well as LHC and LFV searches.

In Section 2 we summarise the basic non-universal features of the GUTs we study that are relevant for our discussion. In Section 3 we discuss different mechanisms for determining the relic density of dark matter (DM) in the presence of non-universal SUSY-breaking mass terms. In Section 4 we discuss lepton flavour mixing effects in the presence of see-saw neutrinos. In Section 5 we look at the branching ratios for rare LFV decays in different DM scenarios, also taking LHC and direct DM searches into account. Finally, our main results and future detection prospects are summarised in Section 6.

2 Non-universal soft supersymmetry breaking in GUT models

In our analysis, we assume that SUSY breaking occurs in a hidden sector at some scale $M_X > M_{GUT}$, via a mechanism that generates flavour-blind soft terms in the visible sector. Between the scales M_X and M_{GUT} , although the theory still preserves the GUT symmetry, quantum corrections may induce non-universalities for soft terms that belong to different GUT representations, while particles that belong to the same representation have common soft masses.

The soft SUSY-breaking scalar terms for the fields in an irreducible representation r of the unification group are parametrised as multiples of a common scale m_0 :

$$m_r = x_r m_0, \quad (1)$$

while the trilinear terms are defined as:

$$A_r = Y_r A_0, \quad A_0 = a_0 m_0, \quad (2)$$

where Y_r is the Yukawa coupling associated with the representation r . We use the standard parametrization with a_0 a dimensionless factor, which we assume to be representation-independent. Since the two Higgs fields of the MSSM arise from different SU(5) representations, they have in general different soft masses. The situation in the different GUT groups is then as follows:

- SU(5): In this case, the multiplet assignments are as follows:

$$(Q, u^c, e^c)_i \in \mathbf{10}_i, \quad (L, d^c)_i \in \bar{\mathbf{5}}_i, \quad \nu_i^c \in \mathbf{1}_i. \quad (3)$$

We assume that the soft terms are the same for all the members of the same representation at the GUT scale, but may be different for the $\mathbf{10}$ and $\bar{\mathbf{5}}$ representations. Here we use as reference the common soft SUSY-breaking masses for the fields of the $\mathbf{10}$, denoted by m_{10} . The masses for the other representations are then defined as:

$$m_{10} = m_0, \quad m_5 = x_5 \cdot m_{10}, \quad m_{H_u} = x_u \cdot m_{10}, \quad m_{H_d} = x_d \cdot m_{10}, \quad (4)$$

and the A terms are specified via a common mass scale:

$$A_{10,5} = a_0 m_0. \quad (5)$$

- Flipped SU(5) (FSU(5)): Since the particle assignments are now different, namely:

$$(Q, d^c, \nu^c)_i \in \mathbf{10}_i, \quad (L, u^c)_i \in \bar{\mathbf{5}}_i, \quad e_i^c \in \mathbf{1}_i, \quad (6)$$

and the parametrisation changes to

$$m_{10} = m_0, \quad m_5 = x_5 \cdot m_{10} \quad m_R = x_R \cdot m_{10} \quad m_{H_u} = x_u \cdot m_{10} \quad m_{H_d} = x_d \cdot m_{10}, \quad (7)$$

where x_R refers to the SU(2)-singlet fields. As previously, the A terms are specified as universal: $A_0 = a_0 \cdot m_0$.

- 4-2-2 symmetry: In this case, a significant modification arises already in the correlation of gaugino masses, since the embedding of the hypercharge generator in the 4-2-2 group implies:

$$M_1 = \frac{3}{5}M_2 + \frac{2}{5}M_3, \quad (8)$$

yielding gluino coannihilations that are absent in models based on other groups [39]. Sfermions are accommodated in 16-dimensional spinor representations, with their common soft mass parameter being m_{16} . The electroweak MSSM doublets lie in the 10-dimensional representation with D-term contributions that split their soft masses: $m_{H_{u,d}}^2 = m_{10}^2 \pm 2M_D^2$. In our notation:

$$x_u = \frac{m_{H_u}}{m_{16}}, \quad x_d = \frac{m_{H_d}}{m_{16}}, \quad (9)$$

with $x_u < x_d$. In the left-right asymmetric 4-2-2 model, a new parameter is introduced:

$$x_{LR} = \frac{m_L}{m_R}, \quad (10)$$

where m_L is the mass of the left-handed sfermions (that preserve the definition of $m_{16} = m_0$), and m_R is the mass of the corresponding right-handed ones.

3 Relic density mechanisms and GUT mass relations

We assume the following relic density constraint [4]:

$$\Omega_\chi h^2 = 0.1186 \pm 0.0031, \quad (11)$$

with a (fixed) theoretical uncertainty of $\tau = 0.012$, (following Refs. [46]) to account for numerical uncertainties in the relic density calculation. This narrow range on the relic density imposes a strong constraint on the DM candidate and the mechanisms that determine its density.

It is well known that particular mass relations must be present in the supersymmetric spectrum if the required amount of relic dark matter is provided by neutralinos. In addition to mass relations, we use the neutralino composition to classify the relevant points of the supersymmetric parameter space. The higgsino fraction of the lightest neutralino mass eigenstate is characterized by the quantity

$$h_f \equiv |N_{13}|^2 + |N_{14}|^2, \quad (12)$$

where the N_{ij} are the elements of the unitary mixing matrix that correspond to the higgsino mass states. Thus, we classify the points that pass the relic density constraint discussed above according to the following criteria:

Higgsino DM:

$$h_f > 0.1, \quad |m_A - 2m_\chi| > 0.1 m_\chi. \quad (13)$$

The first condition in (13) ensures that the lightest neutralino is higgsino-like and, as we discuss later, the lightest chargino χ_1^\pm is almost degenerate in mass with χ_1^0 . The couplings to the SM gauge bosons are not suppressed and χ_1^0 pairs have large cross sections for annihilation into W^+W^- and ZZ pairs, which may reproduce the observed value of the relic DM abundance. Clearly, coannihilation channels involving χ_1^\pm and χ_2^0 also contribute. The second condition in (13) implies that the DM density is not controlled by rapid annihilation through s -channel resonances.

A/H resonances:

$$|m_A - 2m_\chi| \leq 0.1 m_\chi. \quad (14)$$

This condition ensures that the correct value of the relic DM abundance is achieved thanks to s -channel annihilation, enhanced by the resonant heavy neutral Higgs (A and H) propagators. The thermal average $\langle \sigma_{ann} v \rangle$ spreads out the peak in the cross section, so that neutralino masses for which $2m_\chi \simeq m_A$ is not exactly realized can also experience resonant annihilations.

$\tilde{\tau} - \chi_1^0$ coannihilations:

$$h_f < 0.1, \quad (m_{\tilde{\tau}_1} - m_\chi) \leq 0.1 m_\chi \quad (15)$$

The first condition in (15) ensures that the neutralino is bino-like, in which case annihilation into leptons through t -channel slepton exchange is suppressed, and when the second condition in (15) is satisfied coannihilations involving the nearly-degenerate $\tilde{\tau}_1$ enhance the thermal-averaged effective cross section.

$\tilde{\tau} - \tilde{\nu}_\tau - \chi_1^0$ coannihilations:

$$h_f < 0.1, \quad (m_{\tilde{\tau}_1} - m_\chi) \leq 0.1 m_\chi, \quad (m_{\tilde{\nu}_\tau} - m_\chi) \leq 0.1 m_\chi. \quad (16)$$

This is similar to the previous case, but also the $\nu_{\tilde{\tau}}$ is nearly degenerate in mass with the $\tilde{\tau}_1$.

$\tilde{t}_1 - \chi_1^0$ **coannihilations:**

$$h_f < 0.15, \quad (m_{\tilde{t}_1} - m_\chi) \leq 0.1 m_\chi. \quad (17)$$

In this case the \tilde{t}_1 is light and nearly degenerate with the bino-like neutralino. These coannihilations are present in the flipped SU(5) model and in the 4-2-2 model, but not SU(5).

In previous work, we had found that the 4-2-2 model may be distinguished clearly from the other GUT groups, due to the appearance of three additional modes of coannihilation that are not present in other groups:

$\tilde{\chi}^+ - \chi_1^0$ **coannihilations:**

$$h_f < 0.1, \quad (m_{\tilde{\chi}^+} - m_\chi) \leq 0.1 m_\chi. \quad (18)$$

In this case the Higgsino component in the LSP is small, but the lightest chargino is light and nearly degenerate with the bino-like neutralino.

$\tilde{g} - \chi_1^0$ **coannihilations:**

$$h_f < 0.1, \quad (m_{\tilde{g}} - m_\chi) \leq 0.1 m_\chi, \quad (19)$$

In this case the gluino can be relatively light and nearly degenerate with the bino-like neutralino.

$\tilde{b} - \chi_1^0$ **coannihilations:**

$$h_f < 0.1, \quad (m_{\tilde{b}} - m_\chi) \leq 0.1 m_\chi, \quad (20)$$

in this case, in the presence of the LR asymmetry, the \tilde{b} can be light and nearly degenerate with a bino-like neutralino [47].

4 Lepton-flavour mixing effects and see-saw neutrino masses

In what follows, we supplement the previous framework with a see-saw mechanism so as to incorporate neutrino masses [48, 49]. We consider a high-scale see-saw mechanism in which, in order to obtain order 0.1 eV masses for the neutrinos, this scale should be around 10^{14} GeV (assuming electroweak-scale Dirac neutrino masses). Such a mechanism can be realized by extending the MSSM with renormalizable interactions in three scenarios: type I [50] that requires singlet RH neutrinos, type II [51, 52] that requires scalar $SU(2)_L$ triplets and type III [53] that requires fermionic $SU(2)_L$ triplets. Here we focus on the type-I see-saw, in which the additional singlet RH neutrino fields do not affect the running of the

gauge couplings and therefore fit well in our unification schemes. Some examples of the phenomenology of type II and type III models can be found in Refs [54, 55].

We use the following superpotential:

$$W = W_{\text{MSSM}} + Y_\nu^{ij} \epsilon_{\alpha\beta} H_2^\alpha N_i^c L_j^\beta + \frac{1}{2} M_N^{ij} N_i^c N_j^c, \quad (21)$$

where W_{MSSM} is the MSSM superpotential and the N_i^c are additional superfields that contain the three singlet (right-handed) neutrinos, ν_{Ri} , and their scalar partners, $\tilde{\nu}_{Ri}$, and M_N^{ij} denotes the 3×3 Majorana mass matrix for the heavy right-handed neutrinos. The full set of soft SUSY-breaking terms is given by

$$-L_{\text{soft,SI}} = -L_{\text{soft}} + (m_\nu^2)_j^i \tilde{\nu}_{Ri}^* \tilde{\nu}_R^j + \left(\frac{1}{2} B_\nu^{ij} M_N^{ij} \tilde{\nu}_{Ri}^* \tilde{\nu}_{Rj}^* + A_\nu^{ij} h_2 \tilde{\nu}_{Ri}^* \tilde{l}_{Lj} + \text{h.c.} \right), \quad (22)$$

where L_{soft} contains the MSSM soft SUSY-breaking masses, and $(m_\nu^2)_j^i$, A_ν^{ij} and B_ν^{ij} are the new soft SUSY-breaking parameters in the see-saw sector.

The see-saw mechanism yields three heavy neutral mass eigenstates that are mainly right-handed and decouple at a high energy scale, with masses that we denote as M_N . Below this scale, the effective theory contains the MSSM plus a higher-dimensional operator that provides masses for the light neutrinos, which are mainly left-handed:

$$W = W_{\text{MSSM}} + \frac{1}{2} (Y_\nu L H_2)^T M_N^{-1} (Y_\nu L H_2). \quad (23)$$

As the right-handed neutrinos decouple at their respective mass scales, at low energy we have the same particle content and mass matrices as in the MSSM. This framework naturally accommodates neutrino oscillations that are consistent with experimental data [56]. At the electroweak scale an effective Majorana mass matrix for light neutrinos,

$$m_{\text{eff}} = -\frac{1}{2} v_u^2 Y_\nu \cdot M_N^{-1} \cdot Y_\nu^T, \quad (24)$$

arises from the Dirac neutrino Yukawa coupling matrix Y_ν (with entries that can be assumed to be of the same order of magnitude as the charged-lepton and quark Yukawa couplings), and the heavy Majorana masses M_N .

We observe from (21) that we can rotate the fields L_i and N_i^c in such a way that the matrices of the lepton Yukawa couplings, Y_ℓ^{ij} , and of the right-handed neutrinos, M_N^{ij} , become diagonal. However, in this basis, the neutrino Yukawa couplings Y_ν^{ij} are not in general diagonal, giving rise to lepton-flavour-violating (LFV) effects [57, 58, 59, 60, 61, 62, 63]. It is important to note here that lepton-flavour conservation is not a consequence of the SM gauge symmetry, even in the absence of the right-handed neutrinos. Consequently, slepton mass terms can violate lepton-flavour conservation in a manner consistent with the gauge symmetry. Indeed, the scale of LFV can be identified with the EW scale, much lower than the right-handed neutrino scale, M_R , which we assume to be common, for simplicity. In the basis where the charged-lepton Yukawa matrix Y_ℓ is diagonal, the soft slepton mass matrix

acquires corrections that contain off-diagonal contributions from the RGE running from M_{GUT} down to M_R , which are of the following form in the leading-log approximation [64]:

$$\begin{aligned} (m_L^2)_{ij} &\sim \frac{1}{16\pi^2} (6m_0^2 + 2A_0^2) (Y_\nu^\dagger Y_\nu)_{ij} \log\left(\frac{M_{\text{GUT}}}{M_R}\right), \\ (m_e^2)_{ij} &\sim 0, \\ (A_l)_{ij} &\sim \frac{3}{8\pi^2} A_0 Y_{li} (Y_\nu^\dagger Y_\nu)_{ij} \log\left(\frac{M_{\text{GUT}}}{M_R}\right). \end{aligned} \quad (25)$$

Below M_R , the off-diagonal contributions remain almost unchanged. Their magnitude depends on the structure of Y_ν at M_R , in a basis where Y_l and M_N are diagonal. Using the approach of [62, 65] a generic form for Y_ν that contains all neutrino experimental information can be obtained:

$$Y_\nu = \frac{\sqrt{2}}{v_u} \sqrt{M_N^\delta} O_R \sqrt{m_\nu^\delta} U^\dagger, \quad (26)$$

where O_R is a general orthogonal matrix and M_N^δ and m_ν^δ denote the diagonalized heavy and light Majorana neutrino mass matrices, respectively. In this basis the matrix U can be identified with the Pontecorvo-Maki-Nakagawa-Sakata (PMNS) matrix, U_{PMNS} :

$$m_\nu^\delta = U^T m_{\text{eff}} U. \quad (27)$$

Assuming that the observed neutrino oscillations can be attributed to hierarchical neutrino masses, we have $m_\nu^\delta = \text{Diag}(1.1 \cdot 10^{-3}, 8 \cdot 10^{-3}, 5 \cdot 10^{-2})$ eV. For Y_ν couplings of order one, the RH neutrinos can take values as large as 10^{14} GeV. The LFV BR's decrease with the RH neutrino scale. However, the matrix O_R is associated with the flavor structure of the RH neutrino mass matrix, which must be nontrivial so as to provide a scenario for baryogenesis through leptogenesis, which typically requires masses of order $10^8 - 10^9$ GeV [66, 67]. It may also induce cancellations in the LFV BRs that may allow RH neutrino masses above the 10^{14} GeV scale while respecting the current constraints. To illustrate this point, we consider real see-saw parameters and parametrize the matrix O_R with three real angles $\theta_1, \theta_2, \theta_3$, following the notation of Ref. [62]:

$$O_R = R_{12}(\hat{\theta}_3) \cdot R_{13}(\hat{\theta}_2) \cdot R_{23}(\hat{\theta}_1), \quad (28)$$

where

$$R_{23} = \begin{pmatrix} 1 & 0 & 0 \\ 0 & \hat{c}_1 & \hat{s}_1 \\ 0 & \hat{s}_1 & \hat{c}_1 \end{pmatrix}; R_{13} = \begin{pmatrix} \hat{c}_2 & 0 & \hat{s}_2 \\ 0 & 1 & 0 \\ \hat{s}_2 & 0 & \hat{c}_2 \end{pmatrix}; R_{12} = \begin{pmatrix} \hat{c}_3 & \hat{s}_3 & 0 \\ \hat{s}_3 & \hat{c}_3 & 0 \\ 0 & 0 & 1 \end{pmatrix}. \quad (29)$$

We denote $\sin(\hat{\theta}_i)$ and $\cos(\hat{\theta}_i)$ as \hat{s}_i and \hat{c}_i respectively ($i = 1, 2, 3$).

For the matrix U , we consider as an illustrative example the Harrison, Perkins, and Scott (HPS) mixing matrix [68]:

$$U = \begin{pmatrix} \sqrt{\frac{2}{3}} & \frac{1}{\sqrt{3}} & 0 \\ \frac{-1}{\sqrt{6}} & \frac{1}{\sqrt{3}} & \frac{1}{\sqrt{2}} \\ \frac{-1}{\sqrt{6}} & \frac{1}{\sqrt{3}} & \frac{-1}{\sqrt{2}} \end{pmatrix}. \quad (30)$$

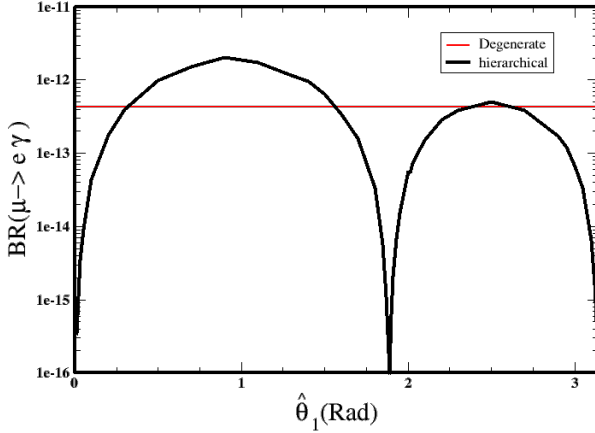


Figure 1: $BR(\mu \rightarrow e\gamma)$ vs $\hat{\theta}_1$ under two different assumptions for the right-handed neutrinos using the CMSSM with $m_0 = 650$ GeV, $m_{1/2} = 700$ GeV, $A_0 = -1400$ GeV and $\tan\beta = 40$, $\mu > 0$ and $M_3 = 2.5 \cdot 10^{12}$ GeV.

trino mass hierarchy, while the BRs are independent of the matrix O_R . In the case of hierarchical RH neutrinos, the matrix Y_ν can have large entries even for the first two generations, increasing the predicted BRs. However, the matrix O_R may induce large cancellations that can result in lower BRs with larger RH neutrino masses and couplings in the case of degenerate RH neutrino masses. This behavior can be understood by comparing the predictions for $BR(\mu \rightarrow e\gamma)$ in the case of degenerate and hierarchical RH neutrinos.

In the case of degenerate right-handed neutrinos ($M_i = M_N$):

$$Y_\nu = Y_0 \sqrt{\frac{m_\nu^\delta}{m_{\nu_3}}} U^\dagger, \quad (31)$$

where $Y_0 = \sqrt{2}/v_u \sqrt{M_N \cdot m_{\nu_3}}$. For the hierarchical case, assuming that $m_{\nu_1} \sim 0$ and that $M_1, M_2 \ll M_3$, using U values from equation (30) and the generic rotation (29), we find that Y_ν only depends on $\hat{\theta}_1$:

$$Y_\nu = \bar{Y}_0 \begin{pmatrix} 0 & 0 & 0 \\ 0 & 0 & 0 \\ \sqrt{\frac{m_{\nu_2}}{m_{\nu_3}}} \cdot \frac{\hat{s}_1}{\sqrt{3}} & \frac{\hat{c}_1}{\sqrt{2}} + \sqrt{\frac{m_{\nu_2}}{m_{\nu_3}}} \cdot \frac{\hat{s}_1}{\sqrt{3}} & -\frac{\hat{c}_1}{\sqrt{2}} + \sqrt{\frac{m_{\nu_2}}{m_{\nu_3}}} \cdot \frac{\hat{s}_1}{\sqrt{3}} \end{pmatrix}. \quad (32)$$

where $Y_0 = \sqrt{2}/v_u \sqrt{M_3 \cdot m_{\nu_3} \cdot \hat{c}_2}$.

Figure 1 shows the prediction for $BR(\mu \rightarrow e\gamma)$ under both assumptions for the right-handed neutrinos, assuming the CMSSM with $m_0 = 650$ GeV, $m_{1/2} = 700$ GeV, $A_0 = -1400$ GeV and $\tan\beta = 40$, $\mu > 0$ and $M_3 = 2.5 \cdot 10^{12}$ GeV. For the case of hierarchical right-handed neutrinos we assume $\cos(\hat{\theta}_2) = 1$. It is easy to conclude that assuming hierarchical light neutrinos and a common scale for the right-handed neutrinos provides a simple benchmark. In this case, using (26), we find

$$Y_\nu^\dagger Y_\nu = \frac{2}{v_u^2} M_R U m_\nu^\delta U^\dagger. \quad (33)$$

In order to determine the slepton mixing parameters, we need a specific form of the product $Y_\nu^\dagger Y_\nu$, shown in (25). Even with the assumption of hierarchical light neutrinos and a fixed U matrix we can still have different predictions for $BR(l_j \rightarrow l_i + \gamma)$ depending on the model used for RH neutrino masses. For instance, in the case of SU(5) models several examples are provided in ref. [57]. The case of degenerate RH neutrinos implies hierarchical Y_ν matrices, since they inherit the neu-

SUSY parameters	4-2-2	SU(5)	FSU(5)
$100 \text{ GeV} \leq m_0 \leq 10 \text{ TeV}$	$0 \leq x_u \leq 2$	$0 \leq x_u \leq 2$	$0 \leq x_u \leq 2$
$50 \text{ GeV} \leq m_{1/2} (M_2 \text{ in 4-2-2}) \leq 10 \text{ TeV}$	$0 \leq x_d \leq 2$	$0 \leq x_d \leq 2$	$0 \leq x_d \leq 2$
$-10 \text{ TeV} \leq A_0 \leq 10 \text{ TeV}$	$0 \leq x_{LR} \leq 2$	$0 \leq x_5 \leq 2$	$0 \leq x_5 \leq 2$
$2 \leq \tan \beta \leq 65$			$0 \leq x_R \leq 2$
$-3000 \text{ GeV} \leq M_3 \text{ (in 4-2-2)} \leq 10 \text{ TeV}$			

Table 1: *Parameter ranges sampled in our scan of the parameter spaces of the GUT models we study.*

Under the assumption of common masses for the heavy Majorana neutrinos, the LFV effects are independent of the matrix O_R . On the other hand, the predicted curve of the hierarchical case in Figure 1 depends on $\hat{\theta}_1$ as $(Y_\nu^\dagger Y_\nu)_{12}^2$, where Y_ν is given in eq. (32).

5 LFV, Dark Matter and the LHC

We perform parameter space scans similar to those in [39, 45, 44], where the initial conditions of the soft terms are determined by a unification group that breaks at M_{GUT} (defined as the scale where the g_1 and g_2 couplings meet, while $g_3(M_{GUT})$ is obtained by requiring $\alpha_s(M_Z) = 0.1187$). For our analysis we use the `SuperBayes` [69, 70, 71], package to perform statistical inference of SUSY models, which is linked to `SoftSusy` [72] to compute the SUSY spectrum, to `MicrOMEGAs` [73] and `DarkSUSY` [74] to compute DM observables, to `SuperIso` [75] to compute flavour physics and the muon anomalous magnetic moment $g-2$. The `MultiNest` [76] algorithm is used to scan the parameter space and identify regions compatible with the data.

We have scanned the parameter spaces of the three GUT groups over the broad ranges of parameters shown in Table 1, including soft SUSY-breaking terms up to 10 TeV, with the results that we now discuss. In addition to the dark matter density constraint mentioned above (11), we impose the following constraints:

$$123 \text{ GeV} \leq m_h \leq 127 \text{ GeV}, \quad (34)$$

which includes an allowance for the theoretical uncertainty in the calculation of m_h in the CMSSM, which is computed using [72]. We extract the following B-physics constraints from [77]:

$$1.1 \times 10^{-9} \leq \text{BR}(B_s \rightarrow \mu^+ \mu^-) \leq 6.2 \times 10^{-9}, \quad (35)$$

which accommodates the range allowed experimentally at the $2\text{-}\sigma$ level,

$$2.99 \times 10^{-4} \leq \text{BR}(B \rightarrow X_s \gamma) \leq 3.87 \times 10^{-4}, \quad (36)$$

which also covers the $2\text{-}\sigma$ experimental range, and

$$0.15 \leq \frac{\text{BR}(B_u \rightarrow \tau \nu_\tau)_{\text{MSSM}}}{\text{BR}(B_u \rightarrow \tau \nu_\tau)_{\text{SM}}} \leq 2.41, \quad (37)$$

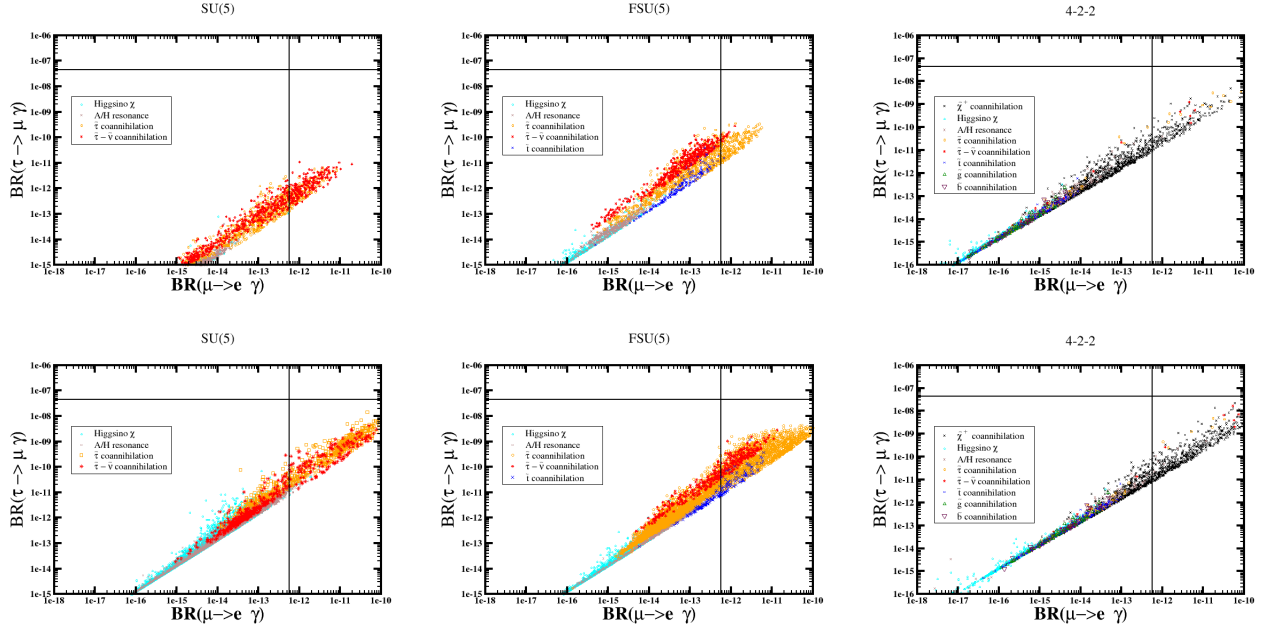


Figure 2: Predictions for $\text{BR}(\tau \rightarrow \mu \gamma)$ and $\text{BR}(\mu \rightarrow e \gamma)$ for (from left to right) the $SU(5)$, $FSU(5)$ and $4-2-2$ models. The upper (lower) panels assume $M_N = 2.5 \cdot 10^{12}$ ($M_N = 10^{13}$ GeV). The symbols correspond to classes of models representing the DM scenarios described in the text, which are indicated in the plot legends.

which covers the $3\text{-}\sigma$ experimental range. These constraints are implemented as described in [71].

In addition, we impose the constraints on the spin-independent (SI) neutralino-nucleon cross-section provided by the LUX [9], Xenon-1T [12] and PandaX experiments [11].

5.1 $\text{BR}(l_i \rightarrow l_j \gamma)$

The processes $l_i \rightarrow l_j \gamma$ with $i \neq j$ are allowed at potentially observable levels in SUSY models with flavour mixing among leptons and their scalar partners. In the CMSSM this mixing does not occur, due to the assumption of universal soft terms at the GUT scale. However, this simple SUSY extension of the SM cannot explain neutrino flavour oscillations and, when the model is supplemented with a mechanism to account for them, flavour oscillations of charged leptons also occur. In the MSSM supplemented by a type-I see-saw as described in the previous Section, which is compatible with the available neutrino data, the uncertainties in the latter may lead to LFV predictions that can differ by several orders of magnitude. Our target in this work, therefore, is not only to analyze the possibility of observing LFV in current experiments, but also to understand the impact of the bounds on $\text{BR}(\mu \rightarrow e \gamma)$ on the perspectives for LHC data. In the simplified see-saw scenario presented in Section 4, we must still specify the following parameters:

- The right-handed neutrino scale, which we assume to be common for all generations.

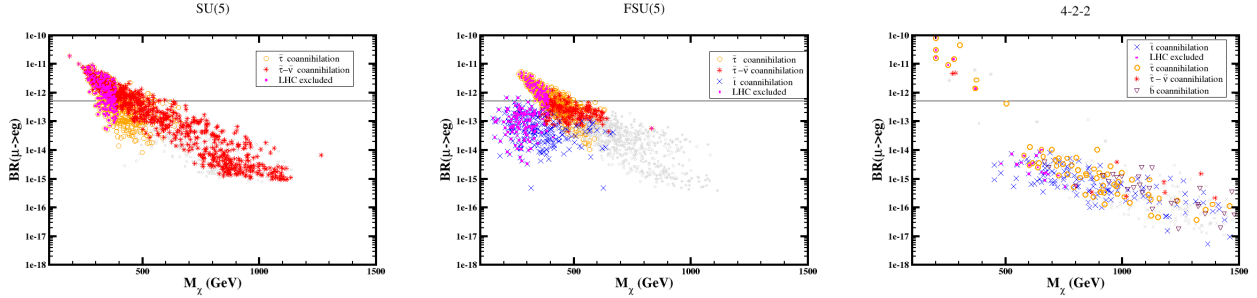


Figure 3: Prediction for $\text{BR}(\mu \rightarrow e\gamma)$ vs m_χ for (from left to right) the $SU(5)$, the $FSU(5)$ and $4-2-2$ models, in scenarios where sfermions coannihilate with the LSP. We use the same notation for the DM models as in Fig. 2. Models with parameters not detectable at the LHC are marked in grey, while excluded models are marked with purple dots. We assume $M_N = 2.5 \cdot 10^{12}$ GeV in all three cases.

- Lepton-slepton mixings parametrized by a matrix similar to the PMNS matrix at the GUT scale. We fix the entries assuming that they are real and that their values are such that the neutrino observables are predicted at their experimental central values. In this simple scheme, the product $Y_\nu^\dagger Y_\nu$ is defined by the PNMS matrix as in (33).
- SUSY soft masses are flavour-independent at the GUT scale. However, we allow the sfermions belonging to different representations of the unification group to have different soft masses.

The first two points are discussed in this Section, as illustrated in Fig. 2, whereas the third point requires a more elaborate treatment, and we dedicate the two subsequent Sections to it.

For fixed light neutrino masses, Eq. (24) links the ratio of the square of the Yukawa couplings to the right-handed neutrino masses. We see that higher right-handed neutrino masses imply, in general, higher Yukawa couplings and larger mixings of the scalar sleptons in Eq. (25), and hence larger LFV branching ratios (BRs). Fig. 2 compares model predictions with the experimental upper limits on $\text{BR}(\tau \rightarrow \mu\gamma)$ and $\text{BR}(\mu \rightarrow e\gamma)$. Comparing the upper and lower panels, we can understand how an increase in M_R by a factor of 4 would imply the exclusion of many models by the current bound on $\text{BR}(\mu \rightarrow e\gamma)$. For the rest of our analysis, we use $M_R = 2.5 \cdot 10^{12}$ GeV. In this case, most of the points that can be explored at the LHC will predict $\text{BR}(\mu \rightarrow e\gamma)$ between the current upper limit and a possible future sensitivity one order of magnitude lower.

The correlation between $\text{BR}(\tau \rightarrow \mu\gamma)$ and $\text{BR}(\mu \rightarrow e\gamma)$ is almost linear, with the prediction of the first being larger than the second by a factor of 10, while the experimental bounds are five orders of magnitude apart. In our study we fixed $Y_\nu^\dagger Y_\nu$ from the PMNS matrix, requiring common right-handed neutrino masses. Although this cannot be considered general, the values of LFV tau decays are maximized by large 2-3 mixing in the PNMS matrix. Furthermore, in $SU(5)$ group symmetries can relate the PMNS and Cabibbo-Kobayashi-Maskawa (CKM) matrix, leading to large mixing in the 2-3 sector. It is nevertheless possible to find particular textures for Y_ν and M_N for which the ratios of μ and τ decays are simultaneously closer to the experimental bounds. These cases will, however, typically

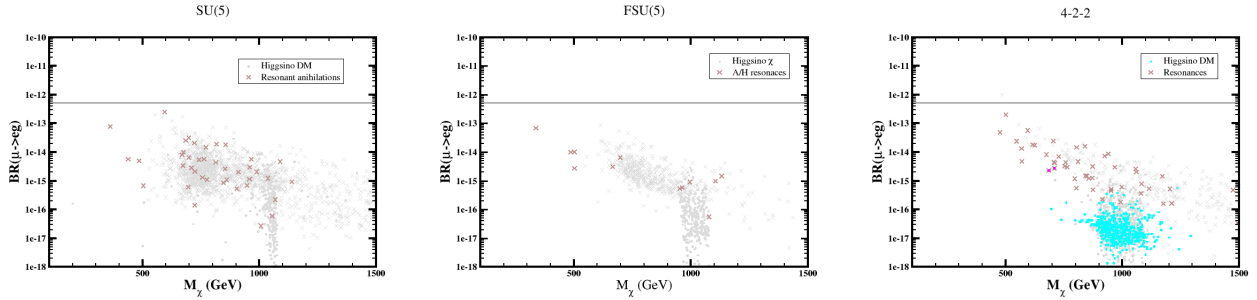


Figure 4: As in Fig. 3, for Higgsino DM and for models of resonant coannihilation.

imply smaller values for the Dirac Yukawa couplings of the first and second generations, predicting less restrictive BRs. Our study can be considered as targeting the kinds of textures that predict large charged LFV.

5.2 Combining $\mu \rightarrow e\gamma$ and LHC bounds

The scale $M_R = 2.5 \cdot 10^{12}$ GeV was chosen as representative. It also turns out that no points are excluded by $\tau \rightarrow \mu\gamma$, since $\mu \rightarrow e\gamma$ is more restrictive. This bound, in combination with large mixing for solar and atmospheric neutrinos, also excludes models with rare τ decays at the levels of the experimental limits in almost all natural textures. Keeping this in mind, we proceed to analyze the predictions for this decay in different unification schemes, studying all kinds of DM models. Since the signal largely depends on the SUSY particle spectroscopy, we combine our analysis with consideration of the LHC data for the specific unified SUSY models under consideration. For this purpose we follow a similar procedure as that applied in Refs. [45, 44]. Each model can be associated to a particular set of particle mass hierarchies and decays, which are then compared with the generic analyses provided by the ATLAS and CMS collaborations [78, 79]. These comparisons are made with the help of Simplified Model Spectra (SMS) which can be defined by a set of hypothetical SUSY particle masses and a sequence of decay patterns that have to be compared with those expected in any specific model. An individual check has to be done for every model, while, due to mismatches between the theoretical predictions and the experimental analyses, it is not possible to provide contour plots where one can easily see which mass ranges are excluded. This task is simplified by using public packages like `Smodels-v1.2.2` [80], which provides a powerful tool for performing a fast analysis of a large number of models [81, 82]. Using this package, the theoretical models are mapped onto SMS and can be compared with the existing LHC bounds if there is a match in the respective topologies. In each model the mass spectrum is generated using `SoftSusy` and the corresponding decay ratios are calculated using `SUSY-HIT` [83]. The cross-section information is then inserted in `Smodels-v1.2.2` through a call to `Pythia 8.2` [84].

We classify the models as follows, according to their LHC prospects:

- (i) Those that are excluded by the current LHC bounds;
- (ii) Those that can be compared with the LHC data and are not excluded;

(iii) Those that cannot be tested at the LHC, i.e., points that predict either processes with very low cross sections or topologies that are not tested at the LHC.

In Fig. 3 and following figures, we denote points of the same DM class with the same symbol as in Fig. 2 but changing the colour according to the LHC prospects of the model: Points of categories (i) and (ii) retain the same colour as in Fig. 2, adding a magenta dot for the excluded ones, whereas points of category (iii) are drawn in grey.

We see in Fig. 3 that the $\mu \rightarrow e\gamma$ bound may be violated in DM models with coannihilations, whereas models with resonant annihilations and higgsino DM are not affected by this bound, as seen in Fig. 4. This can be attributed to the lighter masses of the sleptons in the coannihilation scenarios.

The LHC and charged LFV predictions of models populating classes of points with different DM mechanisms can be compared in the different unification scenarios:

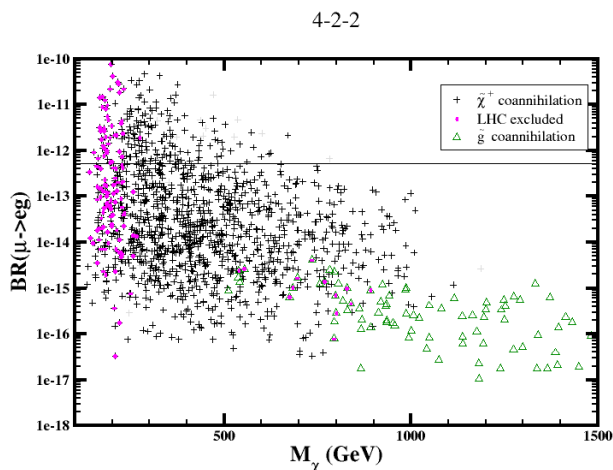


Figure 5: As in Figs. 3 and 4 for models with chargino and gluino coannihilations in the 4-2-2 GUT.

have larger LFV decay rates. As seen in Fig. 4, this scenario is very interesting in SU(5) and FSU(5), since these models predict both LFV and LHC signals within experimental reach. Models with LSP masses above 400 GeV are not excluded in either scenario, but the different representation assignments and hence soft masses change the slepton compositions, with manifest implications for the LFV predictions, which are specific for each group. For instance, whereas in SU(5) most of the points with $\tilde{\tau} - \tilde{\nu} - \chi$ coannihilations violate the experimental bound, in FSU(5) they are still allowed. In the case of 4-2-2 models, there is a left-right splitting of the sfermion soft masses, implying that points with stau coannihilations are more difficult to find than in SU(5), as can be seen in the corresponding panel of Fig.3. Moreover, due to gaugino mass relations, the charginos and neutralinos can be heavier than in SU(5) models, leading to lower $\text{BR}(\mu \rightarrow e\gamma)$.

$\tilde{\tau} - \chi$ and $\tilde{\tau} - \tilde{\nu} - \chi$ coannihilation:

These mechanisms are particularly interesting, since they both predict LFV and LHC signals within experimental reach. In the $\tilde{\tau} - \chi$ scenario, the lighter stau is determined by left-right mixing, and the $\tilde{\tau} - \tilde{\nu} - \chi$ is the limiting case where the $\tilde{\tau}_1$ is mainly left-handed. We should also take into account the fact that LFV is induced mainly in the left-left sector of the slepton mass matrix, due to the see-saw mechanism, therefore models with larger left-stau composition and smaller masses tend to

$\tilde{t} - \chi$ coannihilation: Fig. 4 shows that such models are present in the FSU(5) and in the 4-2-2 schemes, but the predictions are different in the two frameworks. In FSU(5), models with LSP masses up to 700 GeV can predict ratios up to one order of magnitude below the current bound, whereas in 4-2-2 models the LSP mass can be larger, with $\text{BR}(\mu \rightarrow e\gamma)$ two orders of magnitude below the experimental limit.

A/H resonances: As can be seen in Fig. 4, the predictions for LFV decays are below the current limits. However, there are some differences between the three GUTs for the points with good prospects for both the LHC and $\text{BR}(\mu \rightarrow e\gamma)$, which are easier to find in 4-2-2 and SU(5) than in FSU(5).

Higgsino DM: Fig. 4 shows that this class of points does not predict charged LFV of experimental interest, due to the heavy SUSY masses in the three GUT schemes; these models are also out the LHC reach in all SU(5) cases. However, the LSP composition is different in the three schemes; for instance, in the 4-2-2 model the LSP is almost a pure Higgsino and, even if $\text{BR}(\mu \rightarrow e\gamma)$ is low, some model points can be tested at the LHC.

$\tilde{\chi}^+ - \chi$ and $\tilde{g} - \chi$ coannihilations: These DM classes appear only in the 4-2-2 case, due to its GUT relation on gaugino masses. As can be seen in Fig. 5, models with $\tilde{\chi}^+ - \chi$ coannihilations have good detection prospects for both LFV decays and at the LHC. Points with $\tilde{g} - \chi$ coannihilation are still within the LHC reach, while the $\text{BR}(\mu \rightarrow e\gamma)$ predictions are low.

5.3 LFV signals, SUSY spectroscopy and DM detection

In this Section we discuss the LHC prospects for discovering SUSY combined with a possible charged LFV signal. The results are shown in Figs. 6 and 7, which plot SUSY particle masses vs. m_χ , in order to compare directly the range of SUSY masses to which the LHC is sensitive with those that give rise to detectable LFV signatures. In the case of SU(5) and FSU(5), each panel contains all classes of points, while in the 4-2-2 case the different classes are shown in two panels, for clarity of presentation.

We follow the same notation as in the previous Section, with purple dots denoting points excluded by the LHC. In addition to the symbols introduced in the previous Sections, we introduce two more, to show the impact of the LFV predictions on the SUSY spectrum:

- Indigo crosses mark points excluded by the current bound on $\text{BR}(\mu \rightarrow e\gamma)$, and
- Green crosses mark points with predictions for $\text{BR}(\mu \rightarrow e\gamma)$ between the present bound and a factor of 10 below this value.

In addition, the solid red lines are obtained by combining the simplified model bounds from LHC searches. Since these bounds often do not apply directly to our particular cases, this boundary should not be considered as an exclusion line, though excluded points would lie within at least one of these

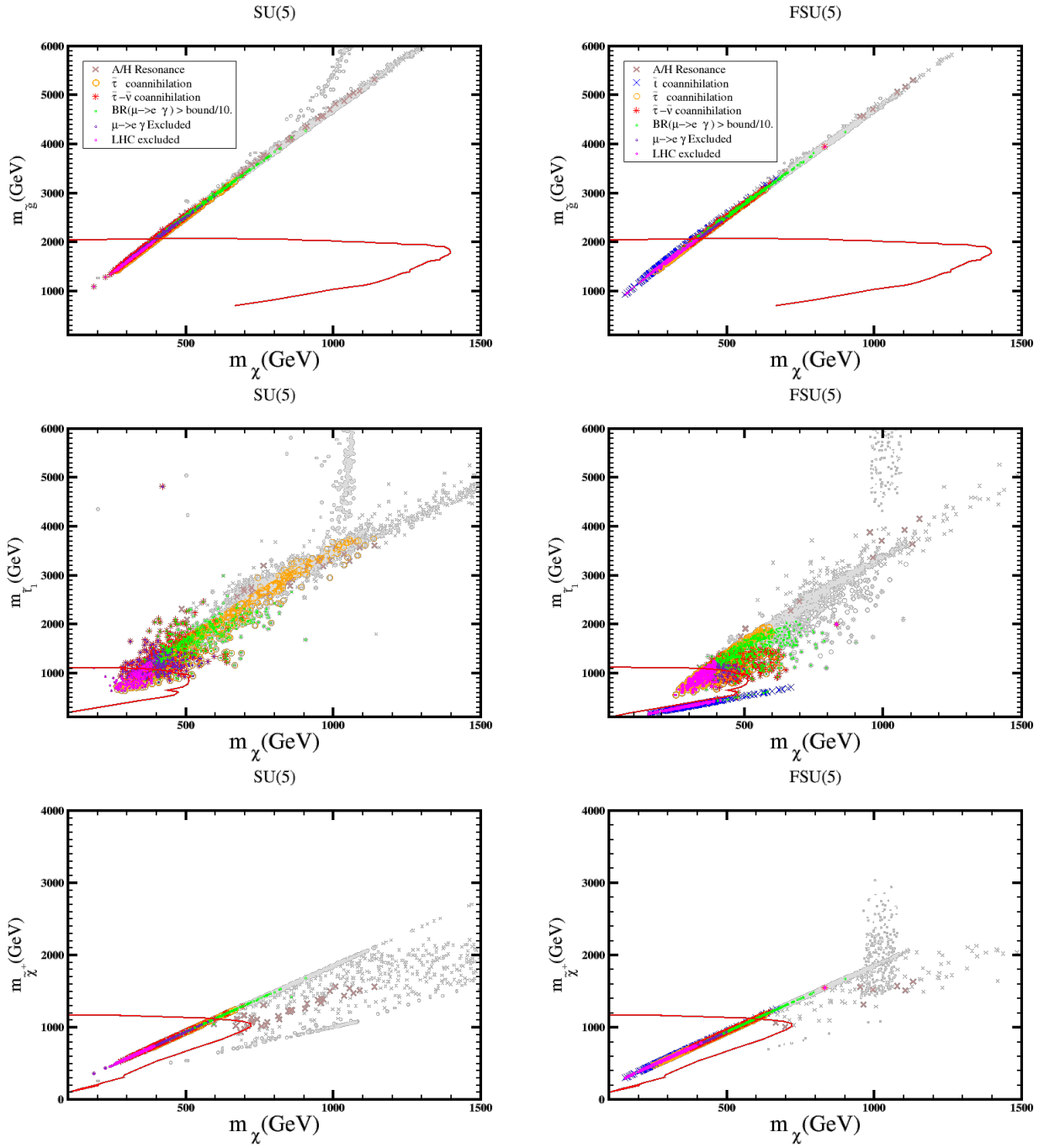


Figure 6: *LHC prospects for the SU5 and FSU5 models. The points follow the notation of Figs. 3, 4 and 5. The meanings of the solid red lines are explained in the text. Indigo crosses indicate points excluded by the limit on $BR(\mu \rightarrow e\gamma)$, whereas the green crosses mark points that lie between the current bound and one order of magnitude below it.*

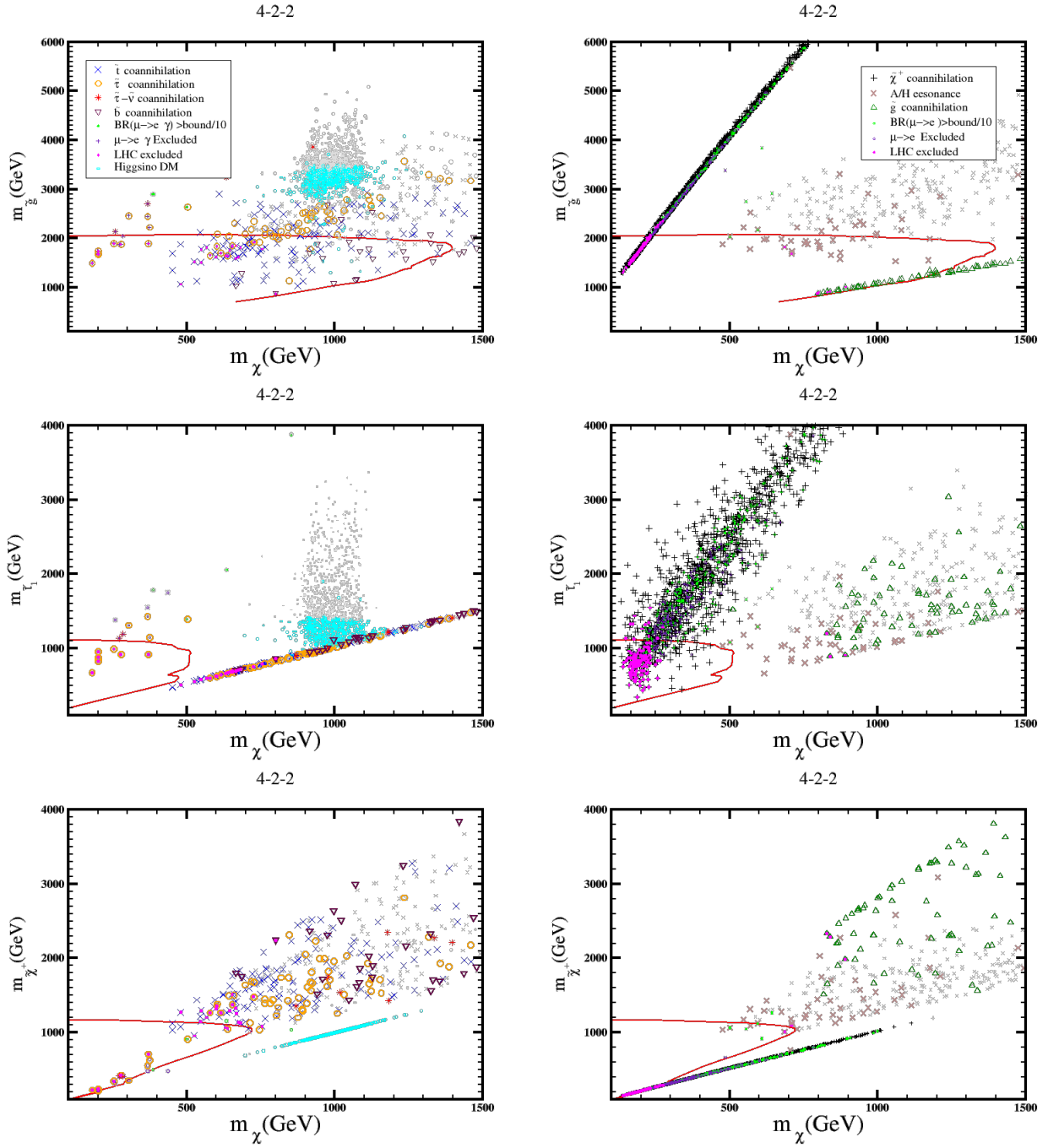


Figure 7: LHC prospects for the 4-2-2 model, following the notations of Fig. 6. For clarity of presentation, in the left panels we display predictions for models with sfermion coannihilations, whereas in the right panels we display the remaining cases.

contours. Nevertheless, it is useful to include this line for illustrative purposes, since it gives an idea of the range of masses explored at the LHC for every SUSY particle.

The upper panels in Fig 6 and 7 display LHC and LFV results on $m_{\tilde{g}} - m_{\chi}$ contour plots. Since in SU(5) and FSU(5) we assume universal gaugino masses at the GUT scale, all except the Higgsino DM models lie on the proportionality lines obtained from the GUT relations. Among other relations, the neutralino mass is in general proportional to that of the gluino, something that does not hold in 4-2-2 where, due to its different group structure, the distribution of models (shown in Fig. 7), follows different patterns. The sfermion coannihilation cases (left panel) do not show any correlation in the $m_{\tilde{g}} - m_{\chi}$ plane. The same holds for models with Higgsino DM and with A/H resonances (right panel), which deviate from the proportionality line. Chargino and gluino coannihilations, on the other hand, display the pattern of mass correlations described in Ref. [44]. We have checked that the excluded points inside the red contour in $m_{\tilde{g}} - m_{\chi}$ plots in Figs. 6 and 7 violate the constraint from the 0-lepton + jets + \cancel{E}_T channel [85, 86]. This bound affects all the models excluded by the LHC in SU(5), and most of the models excluded in the other two scenarios.

Although the superposition of models on Figs. 6 and 7 does not by itself allow a clear distinction among different DM scenarios, we can associate the excluded points to specific models by confronting these figures with the LFV predictions of Figs. 3, 4 and 5. We see that models with sfermion coannihilations in SU(5) and FSU(5) are more affected by the LHC bounds than in the 4-2-2 case, especially for $\tilde{t} - \chi$ coannihilations. In all scenarios, LFV enables exploring a range of $m_{\tilde{g}}$ far beyond the LHC bounds (up to about 4 TeV in SU(5) and FSU(5), and even larger values in 4-2-2 in the chargino coannihilation scenario).

The analysis of excluded models shown in the $m_{\tilde{t}} - m_{\chi}$ plots (middle panels of Figs. 6 and 7) indicates that they are affected by the bound due to searches for stop decays into $t - \chi^{\pm}$ [87, 88, 89, 90]. We see that the exclusion bound in the SU(5) and FSU(5) panels contains many points with slepton coannihilations, while points with $\tilde{t} - \chi$ coannihilations escape this bound. In the case of the 4-2-2 models shown in the left middle panel of Fig. 7, we see that this bound is less effective for the same kind of models than in the other GUTs. In the middle right panel of the same Figure, we see that the bound excludes many models with $\tilde{\chi}^{\pm} - \chi$ coannihilations with m_{χ} below 300 GeV. Regarding LFV, we see that the models present good detection prospects up to stop masses above 3 TeV (and even further in 4-2-2 models). However, in the case of 4-2-2, only models with $\tilde{\chi}^{+} - \chi$ coannihilation predict LFV within one order of magnitude of the current bound.

The $m_{\tilde{\chi}^{\pm}} - m_{\chi}$ plane (bottom panels of Figs. 6 and 7) shows that it is possible to see models excluded by electroweak searches through the ATLAS multi-leptons + \cancel{E}_T channel [91]. This channel is particularly important in models with $\tilde{\chi}^{\pm} - \chi$ coannihilation in the 4-2-2 scenario, where it can exclude models allowed by 0-lepton + jets + \cancel{E}_T . We see that most of the models with chargino mass $m_{\tilde{\chi}^{\pm}} \lesssim 300$ GeV are excluded by these searches. Regarding LFV in SU(5) and FSU(5), we see that the models give rise to good detection prospects for chargino masses up to 1.5 TeV whilst, in the case of 4-2-2, only models with chargino coannihilation present better prospects for LFV detection. In these cases, the masses reach the maximum value of 1 TeV within our data range. The impact is weaker for

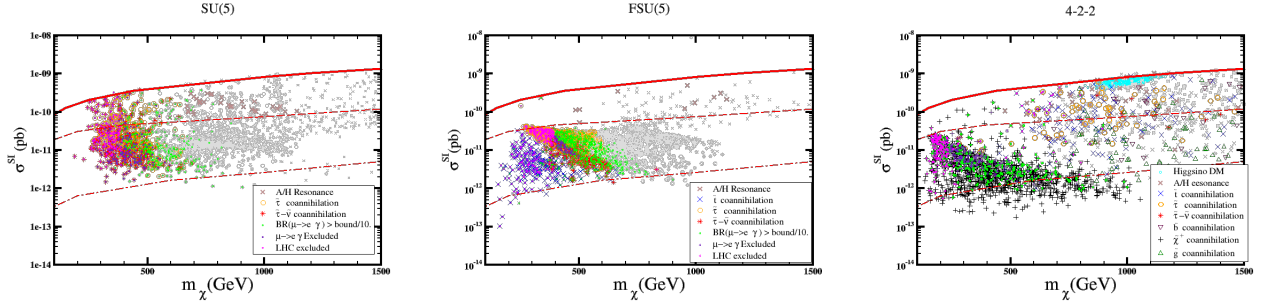


Figure 8: *SI neutralino-nucleon cross section versus m_χ in $SU(5)$, $FSU(5)$ and the 4-2-2 scenarios. The solid lines corresponds to the Xenon-1T bound [12], and the dashed and dot-dashed lines correspond to the projected sensitivities of the LZ [92] and DARWIN [93] experiments.*

sbottom searches, as was shown in [45, 44]. This is due to the fact that in our scenarios the sbottom squarks are heavy and outside the area covered by the LHC; the same happens with signals involving squarks of the lighter generations.

Finally, we display in Fig. 8 the spin-independent (SI) neutralino-nucleon cross section as a function of the neutralino mass in the different GUT models, and we see that the predictions depend on the unification scenario. We note in particular that the FSU(5) model predicts a lower SI cross section than the SU(5) model, in general, while the 4-2-2 model may yield a relatively large SI cross section even for large neutralino masses > 1 TeV. The current bound from the Xenon-1T experiment [12] already excludes many models where the neutralino has a large higgsino component, and the projected sensitivities of the LZ [92] and DARWIN [93] experiments will be able to cover most of the models studied on this work. In particular, only models with $\tilde{\chi}^\pm - \chi$ coannihilations may escape the projected DARWIN sensitivity. Comparing the sensitivities of the LFV, LHC and SI DM searches, we see that the latter are potentially very promising probes of SUSY models. On the other hand, as in [44], we find in each model that the spin-dependent (SD) neutralino-neutron cross section is below the projected limit from the LZ [92] experiment.

6 Conclusions

In previous work, we studied the predictions of different unified theories for DM and the LHC. We investigated several GUT scenarios, comparing the areas allowed within different symmetry schemes. We considered scenarios with gaugino unification, such as SU(5) and FSU(5), and models where it can be relaxed, such as 4-2-2 models. Among others, we had reached the following conclusions:

- Models based on SO(10) are very restricted by data, as can be seen in Refs. [43, 44, 45]. In contrast, SU(5) models contain several areas of interest for higgsino dark matter, resonant annihilations and coannihilations. However, due to its multiplet structure, SU(5) models not allow stop-neutralino coannihilations, in contrast to the other groups.

- Flipped SU(5) models can be clearly distinguished from SU(5), and have several additional features, including stop-neutralino coannihilations.

- Models based on 4-2-2 not only give rise to stop-neutralino and sbottom-neutralino coannihilations, they also allow novel DM mechanisms, including gluino and chargino coannihilations, as a direct consequence of the distinctive gauge structure.

Here we have combined these analyses with the study of LFV, which turns out to be particularly relevant, using updated LHC data. The large mixing for solar and atmospheric neutrinos implies strong correlations between different rare decays. Since the limits for $\mu \rightarrow e\gamma$ are significantly stronger, it made sense to focus mostly on this mode and comment on $\tau \rightarrow \mu\gamma$ where relevant. We have found the following:

- The three groups have distinctive LFV signatures, making it possible to link specific signatures in rare decays and colliders to the gauge and multiplet structure of the theory.

- The results are naturally sensitive to the scale of the right-handed neutrinos, M_R . The see-saw mechanism implies that larger scales are linked to larger couplings and thus larger quantum corrections that violate flavour. For smaller values of M_R the available parameter space is significantly enhanced: indeed, a change of M_R by a factor of 4 is sufficient to exclude or allow a large number of models.

- In all three groups, coannihilations lead to higher rates for LFV, while resonant annihilations and higgsino dark matter are mostly not affected. Overall, in SU(5) and 4-2-2 it is easier to find annihilation models with good detection prospects both at the LHC and in LFV searches. Higgsino DM models do not predict detectable LFV. Still, it is interesting to note that the LSP composition is different in each scheme, yielding an almost pure Higgsino spectrum in the 4-2-2 model.

- Since the see-saw mechanism introduces LFV only in the LL sector, stau coannihilations with smaller masses and larger left-stau components lead to LFV within the current reach. This is particularly relevant for SU(5) and flipped SU(5), since in 4-2-2 models the left-right splitting of the soft fermion masses makes stau coannihilations more difficult to find. However, the two groups can be clearly distinguished, since SU(5) is more restrictive than flipped SU(5).

- Stop-neutralino coannihilations appear only in flipped SU(5) and 4-2-2 models but, once more, with distinct signatures in each case. In 4-2-2 models the LSP can be heavier, and significantly smaller LFV rates are to be expected.

- The 4-2-2 model also allows chargino and gluino coannihilations with neutralinos, due to the different GUT relations for gaugino masses. Chargino-neutralino coannihilations have good detection prospects for both the LHC and LFV, while gluino coannihilations lead to lower LFV rates.

- There are specific correlations between the sparticle masses, leading to interesting signatures. In flipped SU(5), gaugino mass universality results in a proportionality between the gluino and neutralino masses for most of the models under study (corresponding to Higgsino DM and resonant annihilations). Larger masses have good LFV detection prospects, even when they are out of the LHC reach. This is also true for stop-neutralino coannihilations, as well as for models with compressed spectra, such as stau coannihilations.

- In 4-2-2 models, a proportionality relation is found only in chargino-neutralino coannihilations, again due to the GUT relation when the chargino is mostly a Wino. This class of models provides good prospects for both LFV and the LHC, while in other scenarios LFV is significant only for neutralino masses below 500 GeV. This is an additional feature that enables detailed tests of neutralino-chargino coannihilations versus alternative possibilities.

- The experimental advances in direct LSP DM detection are already reaching the sensitivity needed to provide a verdict on many models, specially on the SU(5) and 4-2-2 GUTs. Also, the projected sensitivities of the LZ and DARWIN experiments will provide probes of models that are complementary to LFV searches, even models that cannot be explored at the LHC.

Overall, our results indicate that LFV is a powerful tool that complements LHC and DM searches, and provides valuable information that can help identify optimal modes for future LHC searches. Moreover, not only does it distinguish clearly between various GUTs via the observability of different channels, but it can also provide significant insight into the respective sparticle spectra and neutrino mass parameters.

Acknowledgments

The work of J.E. was supported by the UK STFC Grant ST/P000258/1 and by the Estonian Research Council via a Mobilitas Pluss grant. The research of M.E.G. was supported by the Spanish MINECO, under grant FPA2017-86380. R. RdA acknowledges partial funding/support from the Elusives ITN (Marie Skłodowska-Curie grant agreement No 674896) and the “SOM Sabor y origen de la Materia” (FPA 2017-85985-P). Q.S. acknowledges support by the US DOE grant No. DE-SC0013880.

References

- [1] E. Komatsu *et al.* [WMAP Collaboration], *Astrophys. J. Suppl.* **192** (2011) 18 [arXiv:1001.4538 [astro-ph.CO]].
- [2] C. L. Bennett *et al.* [WMAP Collaboration], *Astrophys. J. Suppl.* **208** (2013) 20 [arXiv:1212.5225 [astro-ph.CO]].
- [3] P. A. R. Ade *et al.* [Planck Collaboration], *Astron. Astrophys.* **571** (2014) A16 [arXiv:1303.5076 [astro-ph.CO]].
- [4] P. A. R. Ade *et al.* [Planck Collaboration], *Astron. Astrophys.* **594** (2016) A13 [arXiv:1502.01589 [astro-ph.CO]].
- [5] G. Aad *et al.* [ATLAS Collaboration], *Phys. Lett. B* **716** (2012) 1 [arXiv:1207.7214 [hep-ex]].

- [6] S. Chatrchyan *et al.* [CMS Collaboration], Phys. Lett. B **716** (2012) 30 [arXiv:1207.7235 [hep-ex]].
- [7] For a compendium of CMS searches for supersymmetry, see <https://twiki.cern.ch/twiki/bin/view/CMSPublic/PhysicsResultsSUS>.
- [8] For a compendium of ATLAS searches for supersymmetry, see <https://twiki.cern.ch/twiki/bin/view/AtlasPublic/SupersymmetryPublicResults>.
- [9] D. S. Akerib *et al.* [LUX Collaboration], Phys. Rev. Lett. **118** (2017) no.2, 021303 [arXiv:1608.07648 [astro-ph.CO]].
- [10] E. Aprile *et al.* [XENON Collaboration], Phys. Rev. Lett. **119** (2017) no.18, 181301/ [arXiv:1705.06655 [astro-ph.CO]]; Phys. Rev. Lett. **121** (2018) no.11, 111302/ doi:10.1103/PhysRevLett.121.111302 [arXiv:1805.12562 [astro-ph.CO]].
- [11] X. Cui *et al.* [PandaX-II Collaboration], Phys. Rev. Lett. **119** (2017) no.18, 181302 doi:10.1103/PhysRevLett.119.181302 [arXiv:1708.06917 [astro-ph.CO]].
- [12] E. Aprile *et al.* [XENON Collaboration], Phys. Rev. Lett. **121** (2018) no.11, 111302 doi:10.1103/PhysRevLett.121.111302 [arXiv:1805.12562 [astro-ph.CO]].
- [13] C. Amole *et al.* [PICO Collaboration], Phys. Rev. Lett. **118** (2017) no.25, 251301 [arXiv:1702.07666 [astro-ph.CO]].
- [14] H. Goldberg, Phys. Rev. Lett. **50** (1983) 1419; J. R. Ellis, J. S. Hagelin, D. V. Nanopoulos, K. A. Olive and M. Srednicki, Nucl. Phys. B **238** (1984) 453. doi:10.1016/0550-3213(84)90461-9
- [15] J. R. Ellis, S. Kelley and Dimitri V. Nanopoulos, Phys. Lett. B249, 441, 1990 and Phys. Lett. B260, 131, 1991; Ugo Amaldi, Wim de Boer, and Hermann Furstenau. Phys. Lett., B260, 447, 1991; Paul Langacker and Ming-xing Luo, Phys. Rev. D44, 817, 1991; C. Giunti, C. W. Kim and U. W. Lee, Mod. Phys. Lett. A6, 1745, 1991.
- [16] F. Borzumati and A. Masiero, Phys. Rev. Lett. **57** (1986) 961. doi:10.1103/PhysRevLett.57.961
- [17] J. Adam *et al.* [MEG Collaboration], arXiv:1303.0754 [hep-ex].
- [18] K. A. Olive *et al.* [Particle Data Group Collaboration], Chin. Phys. C **38**, 090001 (2014).
- [19] I. H. Lee, Phys. Lett. **138B** (1984) 121 and Nucl. Phys. B **246** (1984) 120.
- [20] N. V. Krasnikov, JETP Lett. **65** (1997) 148; S. I. Bitukov and N. V. Krasnikov, arXiv:hep-ph/9806504, (*10th International Seminar on High-Energy Physics Suzdal, Russia*); K. Agashe and M. Graesser, Phys. Rev. D **61** (2000) 075008.
- [21] I. Hinchliffe and F. E. Paige, Phys. Rev. D **63** (2001) 115006;

- [22] J. Hisano, R. Kitano and M. M. Nojiri, Phys. Rev. D **65** (2002) 116002; D.Carvalho, J. Ellis, M. Gómez, S. Lola and J. Romão, Phys. Lett. B **618** (2005) 162.
- [23] A. Bartl, K. Hidaka, K. Hohenwarther-Sodek, T. Kernreiter, W. Majerotto and W. Porod, Eur. Phys. J. C **46**, 783 (2006) [hep-ph/0510074].
- [24] E. Carquin, J. Ellis, M. E. Gómez, S. Lola and J. Rodríguez-Quintero, JHEP **0905** (2009) 026.
- [25] A. Abada, A. J. R. Figueiredo, J. C. Romão and A. M. Teixeira, JHEP **1108** (2011) 099 [arXiv:1104.3962 [hep-ph]].
- [26] J. N. Esteves, J. C. Romão, A. Villanova del Moral, M. Hirsch, J. W. F. Valle and W. Porod, JHEP **0905** (2009) 003 [arXiv:0903.1408 [hep-ph]].
- [27] M. Hirsch, W. Porod, F. Staub and C. Weiss, Phys. Rev. D **87**, 013010 (2013)
- [28] N. Arkani-Hamed, H. Cheng, J. L. Feng and L. J. Hall, Phys. Rev. Lett. **77** (1996) 1937; Nucl. Phys. B **505** (1997) 3.
- [29] J. Hisano, M. M. Nojiri, Y. Shimizu and M. Tanaka, Phys. Rev. D **60**, 055008 (1999);
- [30] M. Guchait, J. Kalinowski and P. Roy, Eur. Phys. J. C **21**, 163 (2001).
- [31] F. Deppisch, J. Kalinowski, H. Päs, A. Redelbach and R. Rückl, arXiv:hep-ph/0401243, work performed for the LHC/LC study group.
- [32] F. Deppisch, H. Päs, A. Redelbach, R. Rückl and Y. Shimizu, Phys. Rev. D **69** (2004) 054014.
- [33] M. Cannoni, C. Carimalo, W. Da Silva and O. Panella, Phys. Rev. D **72** (2005) 115004 [Erratum-ibid. D **72** (2005) 119907] [hep-ph/0508256];
- [34] E. Carquin, J. Ellis, M. E. Gómez and S. Lola, JHEP **1111** (2011) 050.
- [35] A. Abada, A. J. R. Figueiredo, J. C. Romão and A. M. Teixeira, JHEP **1208** (2012) 138 [arXiv:1206.2306 [hep-ph]].
- [36] J. C. Pati and A. Salam, Phys. Rev. D **10**, 275 (1974).
- [37] R.N. Mohapatra and J.C. Pati, Phys. Rev. D **11**, 566 (1975); G. Senjanovic and R.N. Mohapatra, Phys. Rev. D **12**, 1502 (1975); M. Magg, Q. Shafi and C. Wetterich, Phys. Lett. B **87**, 227 (1979);
- [38] G. Lazarides and Q. Shafi, Nucl. Phys. B **189**, 393 (1981); T. W. B. Kibble, G. Lazarides and Q. Shafi, Phys. Lett. B **113**, 237 (1982).
- [39] M. Cannoni, J. Ellis, M. E. G̃şmez, S. Lola and R. Ruiz de Austri, JCAP **1603** (2016) 041 [arXiv:1511.06205 [hep-ph]].
- [40] N. Okada, S. Raza and Q. Shafi, Phys. Rev. D **90** (2014) no.1, 015020 [arXiv:1307.0461 [hep-ph]].

- [41] K. Kowalska, L. Roszkowski, E. M. Sessolo and A. J. Williams, *JHEP* **1506** (2015) 020 [arXiv:1503.08219 [hep-ph]].
- [42] K. Kowalska, L. Roszkowski, E. M. Sessolo and S. Trojanowski, *JHEP* **1404** (2014) 166 [arXiv:1402.1328 [hep-ph]].
- [43] J. Ellis, J. L. Evans, A. Mustafayev, N. Nagata and K. A. Olive, *Eur. Phys. J. C* **76** (2016) no.11, 592 [arXiv:1608.05370 [hep-ph]].
- [44] M. E. Gómez, S. Lola, R. Ruiz de Austri and Q. Shafi, *Front. in Phys.* **6** (2018) 127 doi:10.3389/fphy.2018.00127 [arXiv:1806.11152 [hep-ph]].
- [45] M. E. GÃşmez, S. Lola, R. Ruiz De Austri and Q. Shafi, *JHEP* **1810** (2018) 062 doi:10.1007/JHEP10(2018)062 [arXiv:1806.06220 [hep-ph]].
- [46] L. Roszkowski, E. M. Sessolo and A. J. Williams, *JHEP* **1408** (2014) 067 doi:10.1007/JHEP08(2014)067 [arXiv:1405.4289 [hep-ph]].
- [47] I. Gogoladze, S. Raza and Q. Shafi, *JHEP* **1203** (2012) 054 [arXiv:1111.6299 [hep-ph]].
- [48] L. Calibbi and G. Signorelli, *Riv. Nuovo Cim.* **41** (2018) no.2, 71-174 doi:10.1393/ncr/i2018-10144-0 [arXiv:1709.00294 [hep-ph]].
- [49] A. Vicente, *Adv. High Energy Phys.* **2015** (2015), 686572 doi:10.1155/2015/686572 [arXiv:1503.08622 [hep-ph]].
- [50] P. Minkowski, *Phys. Lett.* **B 67** (1977) 421; M. Gell-Mann, P. Ramond and R. Slansky, in *Complex Spinors and Unified Theories* eds. P. Van. Nieuwenhuizen and D. Freedman, *Supergravity* (North-Holland, Amsterdam, 1979), p.315 [Print-80-0576 (CERN)]; T. Yanagida, in *Proceedings of the Workshop on the Unified Theory and the Baryon Number in the Universe*, eds. O. Sawada and A. Sugamoto (KEK, Tsukuba, 1979), p.95; S. Glashow, in *Quarks and Leptons*, eds. M. Lévy et al. (Plenum Press, New York, 1980), p.687; R. Mohapatra and G. Senjanović, *Phys. Rev. Lett.* **44** (1980) 912; J. Schechter and J. W. F. Valle, *Phys. Rev.* **D 22** (1980) 2227; *Phys. Rev.* **D 25** (1982) 774.
- [51] G. Lazarides, Q. Shafi and C. Wetterich, *Nucl. Phys. B* **181** (1981), 287-300 doi:10.1016/0550-3213(81)90354-0
- [52] R. N. Mohapatra and G. Senjanovic, *Phys. Rev. D* **23** (1981), 165 doi:10.1103/PhysRevD.23.165
- [53] R. Foot, H. Lew, X. G. He and G. C. Joshi, *Z. Phys. C* **44** (1989), 441 doi:10.1007/BF01415558
- [54] J. N. Esteves, J. C. Romao, M. Hirsch, A. Vicente, W. Porod and F. Staub, *JHEP* **12** (2010), 077 doi:10.1007/JHEP12(2010)077 [arXiv:1011.0348 [hep-ph]].

- [55] J. N. Esteves, J. C. Romao, M. Hirsch, W. Porod, F. Staub and A. Vicente, *JHEP* **01** (2012), 095 doi:10.1007/JHEP01(2012)095 [arXiv:1109.6478 [hep-ph]].
- [56] S. Fukuda et al. [Super-Kamiokande Collaboration], *Phys. Rev. Lett.* **86** (2001) 5656 [arXiv:hep-ex/0103033]; *Phys. Rev. Lett.* **86** (2001) 5651 [arXiv:hep-ex/0103032]; *Phys. Lett. B* **539** (2002) 179 [arXiv:hep-ex/0205075]; M. Apollonio et al. [CHOOZ Collaboration], *Phys. Lett. B* **466** (1999) 415 [arXiv:hep-ex/9907037]; Q. Ahmad et al. [SNO Collaboration], *Phys. Rev. Lett.* **87** (2001) 071301 [arXiv:nucl-ex/0106015]; *Phys. Rev. Lett.* **89** (2002) 011301 [arXiv:nucl-ex/0204008]; M. Ambrosio et al. [MACRO Collaboration], *Phys. Lett. B* **517** (2001) 59; G. Giacomelli and M. Giorgini [MACRO Collaboration], arXiv:hep-ex/0110021; K. Eguchi et al. [KamLAND Collaboration], arXiv:hep-ex/0212021.
- [57] M. Cannoni, J. Ellis, M. Gómez and S. Lola, *Phys. Rev. D* **88** (2013) 7, 075005 [arXiv:1301.6002 [hep-ph]].
- [58] M. Gómez, G. Leontaris, S. Lola and J. Vergados, *Phys. Rev. D* **59** (1999) 116009 [arXiv:hep-ph/9810291].
- [59] J. Ellis, M. E. Gómez, G. Leontaris, S. Lola and D. Nanopoulos, *Eur. Phys. J. C* **14** (2000) 319 [arXiv:hep-ph/9911459].
- [60] S. Antusch, E. Arganda, M. Herrero and A. Teixeira, *JHEP* **0611** (2006) 090 [arXiv:hep-ph/0607263].
- [61] J. Ellis, M. Gómez and S. Lola, *JHEP* **0707** (2007) 052 [arXiv:hep-ph/0612292].
- [62] J. Casas and A. Ibarra, *Nucl. Phys. B* **618** (2001) 171 [arXiv:hep-ph/0103065].
- [63] M. E. G \tilde{a} şmez, T. Hahn, S. Heinemeyer and M. Rehman, *Phys. Rev. D* **90** (2014) no.7, 074016 doi:10.1103/PhysRevD.90.074016 [arXiv:1408.0663 [hep-ph]].
- [64] J. Hisano, T. Moroi, K. Tobe and M. Yamaguchi, *Phys. Rev. D* **53** (1996) 2442.
- [65] M. E. Gomez, S. Heinemeyer and M. Rehman, *Eur. Phys. J. C* **75** (2015) no.9, 434 doi:10.1140/epjc/s10052-015-3654-8 [arXiv:1501.02258 [hep-ph]].
- [66] W. Buchmuller, P. Di Bari and M. Plumacher, *Annals Phys.* **315** (2005), 305-351 doi:10.1016/j.aop.2004.02.003 [arXiv:hep-ph/0401240 [hep-ph]].
- [67] C. S. Fong, E. Nardi and A. Riotto, *Adv. High Energy Phys.* **2012** (2012), 158303 doi:10.1155/2012/158303 [arXiv:1301.3062 [hep-ph]].
- [68] P. F. Harrison, D. H. Perkins and W. G. Scott, *Phys. Lett. B* **530** (2002), 167 doi:10.1016/S0370-2693(02)01336-9 [arXiv:hep-ph/0202074 [hep-ph]].

- [69] G. Bertone, D. G. Cerdeno, M. Fornasa, R. Ruiz de Austri, C. Strece and R. Trotta, JCAP **1201** (2012) 015 [arXiv:1107.1715 [hep-ph]].
- [70] C. Strece, G. Bertone, F. Feroz, M. Fornasa, R. Ruiz de Austri and R. Trotta, JCAP **1304** (2013) 013 [arXiv:1212.2636 [hep-ph]].
- [71] G. Bertone, F. Calore, S. Caron, R. R. de Austri, J. S. Kim, R. Trotta and C. Weniger, arXiv:1507.07008 [hep-ph].
- [72] B. C. Allanach, Comput. Phys. Commun. 143 (2002) 305 [hep-ph/0104145]; <http://projects.hepforge.org/softsusy/>.
- [73] G. Belanger, F. Boudjema, A. Pukhov and A. Semenov, Comput. Phys. Commun. 176 (2007) 367; <http://lapth.in2p3.fr/micromegas/>.
- [74] P. Gondolo, J. Edsjo, P. Ullio, L. Bergstrom, M. Schelke and E. A. Baltz, JCAP 0407 (2004) 008; <http://www.darksusy.org/>.
- [75] F. Mahmoudi, Comput. Phys. Commun. 178 (2008) 745 and Comput. Phys. Commun. 180 (2009) 1579
- [76] F. Feroz and M. P. Hobson, Mon. Not. Roy. Astron. Soc. **384** (2008) 449–463; F. Feroz, M. P. Hobson and M. Bridges, Mon. Not. Roy. Astron. Soc. **398**, 1601 (2009) [0809.3437]; <http://www.ft.uam.es/>.
- [77] Y. S. Amhis *et al.* [HFLAV Collaboration], arXiv:1909.12524 [hep-ex]. <https://hflav.web.cern.ch/>
- [78] H. Okawa [ATLAS Collaboration], arXiv:1110.0282 [hep-ex].
- [79] S. Chatrchyan *et al.* [CMS Collaboration], Phys. Rev. D **88** (2013) no.5, 052017 doi:10.1103/PhysRevD.88.052017 [arXiv:1301.2175 [hep-ex]].
- [80] F. Ambrogio *et al.*, doi:10.1016/j.cpc.2019.07.013 arXiv:1811.10624 [hep-ph].
- [81] S. Kraml, S. Kulkarni, U. Laa, A. Lessa, W. Magerl, D. Proschofsky-Spindler and W. Waltenberger, Eur. Phys. J. C **74** (2014) 2868 doi:10.1140/epjc/s10052-014-2868-5 [arXiv:1312.4175 [hep-ph]].
- [82] F. Ambrogio, S. Kraml, S. Kulkarni, U. Laa, A. Lessa and W. Waltenberger, Eur. Phys. J. C **78** (2018) no.3, 215 doi:10.1140/epjc/s10052-018-5660-0 [arXiv:1707.09036 [hep-ph]].
- [83] A. Djouadi, M. M. Muhlleitner and M. Spira, Acta Phys. Polon. B **38** (2007) 635 [hep-ph/0609292].
- [84] T. Sjöstrand *et al.*, Comput. Phys. Commun. **191** (2015) 159 doi:10.1016/j.cpc.2015.01.024 [arXiv:1410.3012 [hep-ph]].

- [85] A. M. Sirunyan *et al.* [CMS Collaboration], Phys. Rev. D **96** (2017) no.3, 032003 [arXiv:1704.07781 [hep-ex]].
- [86] A. M. Sirunyan *et al.* [CMS Collaboration], Eur. Phys. J. C **77** (2017) no.10, 710 [arXiv:1705.04650 [hep-ex]].
- [87] G. Aad *et al.* [ATLAS Collaboration], JHEP **1409** (2014) 176 [arXiv:1405.7875 [hep-ex]].
- [88] A. M. Sirunyan *et al.* [CMS Collaboration], JHEP **1710** (2017) 005 [arXiv:1707.03316 [hep-ex]].
- [89] A. M. Sirunyan *et al.* [CMS Collaboration], Phys. Rev. D **97** (2018) no.1, 012007 [arXiv:1710.11188 [hep-ex]].
- [90] A. M. Sirunyan *et al.* [CMS Collaboration], JHEP **1710** (2017) 019 doi:10.1007/JHEP10(2017)019 [arXiv:1706.04402 [hep-ex]].
- [91] A. M. Sirunyan *et al.* [CMS Collaboration], JHEP **1803** (2018) 160 [arXiv:1801.03957 [hep-ex]].
- [92] D. S. Akerib *et al.* [LUX-ZEPLIN Collaboration], arXiv:1802.06039 [astro-ph.IM].
- [93] J. Aalbers *et al.* [DARWIN Collaboration], JCAP **1611** (2016) 017 doi:10.1088/1475-7516/2016/11/017 [arXiv:1606.07001 [astro-ph.IM]].